Heliyon 10 (2024) e28409

Contents lists available at ScienceDirect

Heliyon

journal homepage: www.cell.com/heliyon

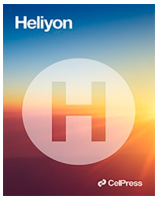

Research article

Bioinformatics analysis and validation of genes related to paclitaxel's anti-breast cancer effect through immunogenic cell death

Qianmei Yang [a,b,*], Guimei Yang [a,b], Yi Wu [c], Lun Zhang [a], Zhuoyang Song [d], Dan Yang [a]

[a] School of Pharmaceutical Science & Yunnan Provincial Key Laboratory of Pharmacology for Natural Products, Kunming Medical University, Kunming, Yunnan, 650500, PR China
[b] Yunnan College of Modern Biomedical Industry, Kunming, Yunnan, 650500, PR China
[c] Science and Technology Achievement Incubation Center, Kunming Medical University, Kunming, Yunnan, 650500, PR China
[d] School of Pharmaceutical Sciences, Wenzhou Medical University, Wenzhou, Zhejiang, 325035, PR China

ARTICLE INFO

Keywords:
Breast cancer
Immunogenic cell death
Paclitaxel
Biomarkers
Prognosis

ABSTRACT

Research indicated that Paclitaxel (PTX) can induce immunogenic cell death (ICD) through immunogenic modulation. However, the combination of PTX and ICD has not been extensively studied in breast cancer (BRCA). The TCGA-BRCA and GSE20685 datasets were enrolled in this study. Samples from the TCGA-BRCA dataset were consistently clustered based on selected immunogenic cell death-related genes (ICD-RGs). Next, candidate genes were obtained by overlapping differentially expressed genes (DEGs) between BRCA and normal groups, intersecting genes common to DEGs between cluster1 and cluster2 and hub module genes, and target genes of PTX from five databases. The univariate Cox algorithm and the least absolute shrinkage and selection operator (LASSO) were performed to obtain biomarkers and build a risk model. Following observing the immune microenvironment in differential risk subgroups, single-gene gene set enrichment analysis (GSEA) was carried out in all biomarkers. Finally, the expression of biomarkers was analyzed. Enrichment analysis showed that 626 intersecting genes were linked with inflammatory response. Further five biomarkers (CHI3L1, IL18, PAPLN, SH2D2A, and UBE2L6) were identified and a risk model was built. The model's performance was validated using GSE20685 dataset. Furthermore, the biomarkers were enriched with adaptive immune response. Lastly, the experimental results indicated that the alterations in IL18, SH2D2A, and CHI3L1 expression after treatment matched those in the public database. In this study, Five PTX-ICD-related biomarkers (CHI3L1, IL18, PAPLN, SH2D2A, and UBE2L6) were identified to aid in predicting BRCA treatment outcomes.

1. Introduction

Breast cancer (BRCA) remains a major epidemiologic challenge, it has become the number one killer threatening women's health [1–3]. Approximately 1 in 8 women will be diagnosed with invasive BRCA in their lifetime, and 1 in 39 women will die from BRCA

* Corresponding author. School of Pharmaceutical Science & Yunnan Provincial Key Laboratory of Pharmacology for Natural Products, Kunming Medical University, Kunming, Yunnan, 650500, PR China.

https://doi.org/10.1016/j.heliyon.2024.e28409
Received 28 September 2023; Received in revised form 14 March 2024; Accepted 18 March 2024
Available online 21 March 2024

[3–5]. BRCA is a complex disease influenced by both genetic and environmental factors, contributing to its heterogeneity, which is related to family genetic susceptibility and personal physique [3,4,6,7]. The age of 40–60 is the age of high incidence of BRCA, and the incidence of BRCA with family history of BRCA is relatively high [3,4,6]. At present, the clinical molecular classification of BRCA is luminal typing, which is determined by four factors: estrogen (ER), progesterone (PR), Human epidermal growth factor receptor-2 (HER2) and Ki-67 index. It can be divided into four types: among them, ER and PR are positive, HER2 is negative, Ki-67 is less than 14%, which is called type A; ER, PR positive, HER2 negative, Ki-67 greater than 14%, is called type B; ER, PR and HER are all negative, which is called triple negative BRCA; and another type is called HER2 over-expression type.

BRCA prognosis and treatment decisions often rely on tumor-node metastasis staging [4,8,9]. Lobular carcinoma in situ at Stage 0 typically does not require treatment, whereas ductal carcinoma in situ may advance to invasive cancer. Treatment options for invasive cancer include breast-conserving surgery and radiotherapy. Breast-conserving surgery and radiotherapy are effective treatments for Stage I and II BRCA, significantly reducing mortality and recurrence rates. Systemic adjuvant therapy selection is influenced by factors such as lymph node involvement, hormone receptor status, HER2 overexpression, patient age, and menopausal status. Typically, node-positive BRCA cases are managed with systemic chemotherapy, endocrine therapy for hormone receptor-positive cancers, and trastuzumab for cancers overexpressing HER2. Most of the chemotherapy schemes are based on anthracycline and PTX [8–10]. A study on the target of radiotherapy response-related genes pointed out that the radiotherapy response-related genes based on differential expression of prognosis can be used to classify the radiotherapy sensitivity and drug resistance clusters in TCGA-BRCA cohort, which can be used to evaluate the radiosensitivity of individual BRCA patients, and the possibility of synergistic effect between radiotherapy and immune checkpoint inhibitors is expounded [11].

Immunogenic cell death (ICD) can trigger cell death that is identifiable by the immune system [12–14]. Tumor cells undergoing ICD are more readily engulfed by antigen-presenting cells, leading to antigen presentation, activation of T cells, and the initiation of a systemic antitumor immune response. A key feature of ICD is its ability to be recognized by the immune system, primarily through the translocation of calreticulin (CRT) to the cell membrane. While cisplatin (CDDP) can recruit myeloid cells to the tumor and support the activation of tumor-specific $CD8^+$ T cells [15] and enhance the effects of vaccines in promoting tumor cell death [16], it does not induce CRT exposure [17]. Combining cisplatin with CRT protein [17] or ER stress inducers like thapsigargin or tunicamycin [18] can restore the immunogenicity of cisplatin-induced cancer cell death. Additionally, several long-standing antitumor agents such as radiotherapy, cyclophosphamide, oxaliplatin (OXP), and cetuximab are known inducers of ICD [17,19,20]. Our previous research confirmed that PTX is a genuine inducer of ICD in various mouse and human tumor cell lines. This was demonstrated by the increased levels of CRT, ERp57, ATP, and HMGB1 [21]. Our research demonstrated that nanomicelle encapsulation could safeguard the effects of ICD by minimizing immune system side effects. This approach offers the potential to achieve both immediate tumor reduction through direct tumor destruction and sustained immune activation for long-term benefits in chemotherapy [21]. The immune-activating potential of ICD is appealing, but it can also contribute to rapid relapse post-chemotherapy. This is because many ICD inducers are cytotoxic agents that not only target tumors but also cause significant harm to the immune system. As a result, the immune-activating aspect of ICD is often downplayed and weakened in cancer treatment strategies [12–14]. At the same time, in clinical BRCA cases, the detailed molecular mechanism of PTX-induced ICD effect is not very clear, which is also one of the obstacles to clinical application. In the case of poor effects of targeted tumor metabolic therapy and immunotherapy, the combination therapy with other drugs, that is, by optimizing pharmacokinetics and adjusting available chemotherapy according to molecular characteristics, is a promising research approach [22].

In our research, we executed a comprehensive analysis of transcriptome data from the Gene Expression Omnibus (GEO) and The Cancer Genome Atlas (TCGA) databases to identify five potential biomarkers for BRCA. Except for IL-18, other key genes were reported for the first time in the research of BRCA prognosis. A risk model of BRCA patients based on PTX and ICD-related genes was constructed, which provided a new reference for the treatment of BRCA, and also provided a basis for explaining the molecular mechanism of ICD induced by PTX. On the basis of genes related to ICD therapy, our research combined with specific drug targets to screen key genes in order to promote clinical practice.

2. Materials and methods

2.1. Source of data

The TCGA-BRCA dataset (training set) including the RNA-seq data from 1072 BRCA samples (1050 BRCA samples had survival information and clinical indicators) and 99 normal samples was acquired from the UCSC Xene database (https://xenabrowser.net). The GSE20685 dataset (GPL570), including the RNA-seq, survival information and clinical indicators data of BRCA tissue from 327 BRCA cohorts, was acquired from the GEO database (https://www.ncbi.nlm.nih.gov/gds) and regarded as an external validation cohort. Then, 34 ICD-related genes (ICD-RGs) were obtained from previous report [23].

2.2. Screening for differentially expressed genes (DEGs) and identify subtypes

DEGs between the BRCA and normal were selected the edgeR package (v 3.36.0) [24] according to adjusted $P < 0.05$ and $|\log_2 FC| > 0.5$ where the generalized linear model (GLM) and the 'glmLRT' function were conducted to flexibly adjust the sample design matrix to adapt to the unbalanced sample size between the BRCA (1072) and normal samples (99) [25]. The findings were visualized using volcano plots and heatmaps. The consistency clustering analysis was then executed on the BRCA samples from TCGA-BRCA dataset on the basis of ICD-RGs using the ConsensusClusterPlus package (v 1.54.0) [26]. Immediately after, principal component analysis (PCA)

plots and K-M survival curves were plotted between different subgroups.

2.3. Identification of DEGs between the Cluster1 and Cluster2

We used the edgeR package (v 3.36.0) to identify DEGs between Cluster1 and Cluster2 [24] with adjusted $P < 0.05$ and $|\log_2 FC| > 0.5$. We used volcano plots and heatmaps to display the results.

2.4. Screening for key module genes by weighted gene co-expression network analysis (WGCNA)

The ICD scores were computed for each sample in the TCGA-BRCA dataset via ssGSEA algorithm and were considered as the clinical traits for the construction of co-expression network by WGCNA [27]. Firstly, the hierarchical clustering was utilized to cluster samples and assess the presence of any outlier samples that display unusual or deviant expression patterns compared to the majority of samples, where the distance matrix is used to measure the similarity between samples. Then, we selected the optimal soft threshold (β) to achieve a network that approximates a scale-free distribution. Subsequently, the cluster dendrogram were obtained by calculating adjacency and similarity. The modules were then partitioned using a dynamic tree cutting algorithm (minModuleSize = 70). Next, we used the ICD score as the trait data to filter relevant module genes. We identified the key module with the highest relevance to the score by creating a module-trait correlation heatmap, and selected the genes in this key module for further analysis.

2.5. Screening and functional enrichment of intersecting genes

The intersecting genes (ICD-genes) were filtered by overlapping key module genes and DEGs between the Cluster1 and Cluster2. Gene Ontology (GO) and the Kyoto Encyclopedia of Genes and Genomes (KEGG) enrichment analysis of intersecting genes was executed via DAVID (v 6.8.0) [28]. Subsequently, the top 10 results for each of GO and KEGG were selected for presentation.

2.6. Identification of target genes

Firstly, the targets for PTX were searched using PTX as the keyword through the Drugbank (https://go.drugbank.com/), herb (http://herb.ac.cn/), CTD (http://ctdbase.org/), and batman (http://bionet.ncpsb.org.cn/batman-tcm/) databases. The targets for PTX were obtained from the PubChem database (https://pubchem.ncbi.nlm.nih.gov/) using "Compound CID: 36314" as search criteria. Finally, the targets acquired from the five databases were combined to obtain the PTX target genes (target genes).

2.7. Screening for candidate genes and construction of risk model

We identified candidate genes by finding the overlapping intersection of genes, target genes and DEGs between the BRCA and normal. The univariate Cox algorithm [29] was conducted for candidate genes to acquire survival-related feature genes. Afterwards, least absolute shrinkage and selection operator (LASSO) analysis (known as L1 regularization) was performed to solve the multi-collinearity problem of various influencing feature genes and reduce the number of covariates in the Cox regression [30,31] The selected genes were utilized as biomarkers for this study, further, their expressions were extracted from the TCGA-BRCA dataset and compared using the Wilcoxon rank sum test. The results were presented by box plot and drawn by ggplot2 package (v 3.3.5) [32].

Next, patients were divided into high- and low-risk groups based on the median values of the risk scores calculated from the biomarkers. Riskscore = ($Coef_i$ represents the regression coefficient of the i th gene, x_i represents the expression value of the i th gene, and n represents the number of biomarkers). Kaplan-Meier (K-M) survival curves were plotted. The survivalROC package (v 1.0.3) [33] was utilized to compute the area under the curve (AUC) values for receiver operating characteristic (ROC) curves to assess the predictive accuracy of the model. The risk model was verified with an external validation cohort (GSE20685 dataset). Besides, clinical information of the cohorts in TCGA-BRCA dataset was extracted for detecting the survival difference using K-M analysis.

2.8. Immune microenvironment analysis

We used the CIBERSORT algorithm to calculate the proportions of 22 immune cell subtypes for each of the 1050 BRCA samples in the TCGA-BRCA dataset [34]. The difference in scores for each immune cell between two differential risk subgroups was compared by Wilcoxon rank sum test after excluding samples with $P > 0.05$. Subsequently, we analyzed the correlation between biomarkers and differential immune cells using the Spearman method. Finally, the scatter plots were plotted to show the two sets of relationships with the strongest positive and negative correlations respectively.

2.9. Single-gene gene set enrichment analysis (GSEA) analysis

In this study, single-gene GSEA analysis (GO-BP and KEGG) was executed using clusterProfiler [35], and the top 5 most significant results for each biomarker were visualized individually.

2.10. Construction of a ceRNA regulatory network

The miRWalk3.0 and miRDB databases were used to predict miRNAs targeting biomarkers. Targeting relationships between lncRNAs and miRNAs were predicted by the LncBaseV2.0 database (score = 1). Finally, using Cytoscape software (v 3.6.1) [36], the lncRNA-miRNA-mRNA network was established.

2.11. qRT-PCR

We collected twenty frozen mouse tissues, including 10 PTX-treated samples and 10 control (BRCA) samples. Total RNA from the 20 samples were extracted with the TRIzol reagent (Ambion, USA) according to the manufacturer's protocol. The cDNA synthesis was reverse-transcribed using the SureScript First-strand cDNA Synthesis kit (Servicebio, China). The qRT-PCR assay was performed with CFX Connect Thermal Cycler (Bio-Rad, USA). The relative quantification of mRNAs was calculated using the $2^{-\Delta\Delta CT}$ method [37]. All primers sequence information were shown in Table 1. Graphpad Prism 5 was utilized for graph creation and p-value calculation.

2.12. Statistical analysis

All bioinformatics analyses were executed using R language, and the data from different groups were compared using the Wilcoxon rank sum test. Spearman method was used to conduct the correlation analysis.

3. Results

3.1. Identification of DEGs and subtypes analysis

A sum of 4876 DEGs were identified between the BRCA and normal groups, comprising 2466 up-regulated genes and 2410 down-regulated genes (Fig. 1A), and the expression heatmap of DEGs were exhibited in Fig. 1B. The consistency clustering results indicated that the samples were classified into two subtypes (Cluster1 and Cluster2) with clear discrimination between the subtypes (Fig. 1C–F). The survival analysis curves demonstrated that Cluster2 had a higher survival rate (Fig. 1G).

3.2. Filtering of DEGs between the Cluster1 and Cluster2 and key module genes

In total, the volcano map of 1119 DEGs between the two Cluster were generated (Fig. S1A) and the expression pattern of which was showed as a heatmap in Fig. S1B. The ICD scores exhibited a obvious difference between the BRCA and normal groups based on the Wilcoxon rank sum test comparison (Fig. S2A). After the ICD scores were computed by the ssGSEA algorithm, WGCNA was performed. Sample clustering results showed there were no outliers (Fig. S2B). When using a soft threshold of 7 ($R^2 = 0.85$, indicated by the blue line), the average connectivity approached 0. (Fig. S2C). A total of 19 modules were initially acquired. Subsequently, by setting the MEDissThres to 0.3 for merging similar modules, the number of modules was reduced to 16 (Fig. S2D). According to the module-trait correlation heatmap, MEmagenta ($Cor = 0.91$, $P \leq 0.05$) had the highest correlation, hence 1148 genes were considered as key module genes (Fig. S2E).

3.3. Screening and functional enrichment of 626 intersecting genes

After intersecting the DEGs between Cluster1 and Cluster2 with the key module genes, totally 626 intersecting genes were identified (Fig. 2A). The enrichment analysis results revealed that the intersecting genes were linked with 609 GO entries and 68 KEGG pathways. Specifically, the GO-BP category encompassed functions such as innate immune response and inflammatory response, while the GO-CC category included terms like immunological synapse and MHC class II protein complex. Additionally, the GO-MF category

Table 1
The primer informations in the quantitative real-time polymerase chain reaction (qRT-PCR).

Gene	Primer sequences
CHI3L1 F	AGACGCCATCCAACCTTTCC
CHI3L1 R	GTTCGACTCGTCATTCCACTC
IL18 F	TCAGACAACTTTGGCCGACT
IL18 R	GGTGGATCCATTTCCACTTTGA
PAPLN F	GGCTTTCGTAGTCGGTGC
PAPLN R	ATTTCGAGCCCAAGACCCTG
SH2D2A F	GCTCAAGACTGCCCCTCTTT
SH2D2A R	ACTTGCCATTTCTTCCCCCA
UBE2L6 F	GAAGCTCACCCTGTGCCTAA
UBE2L6 R	AGGGAAGGAGCACACATCAC
GAPDH F	CCTTCCGTGTTCCTACCCC
GAPDH R	GCCCAAGATGCCCTTCAGT

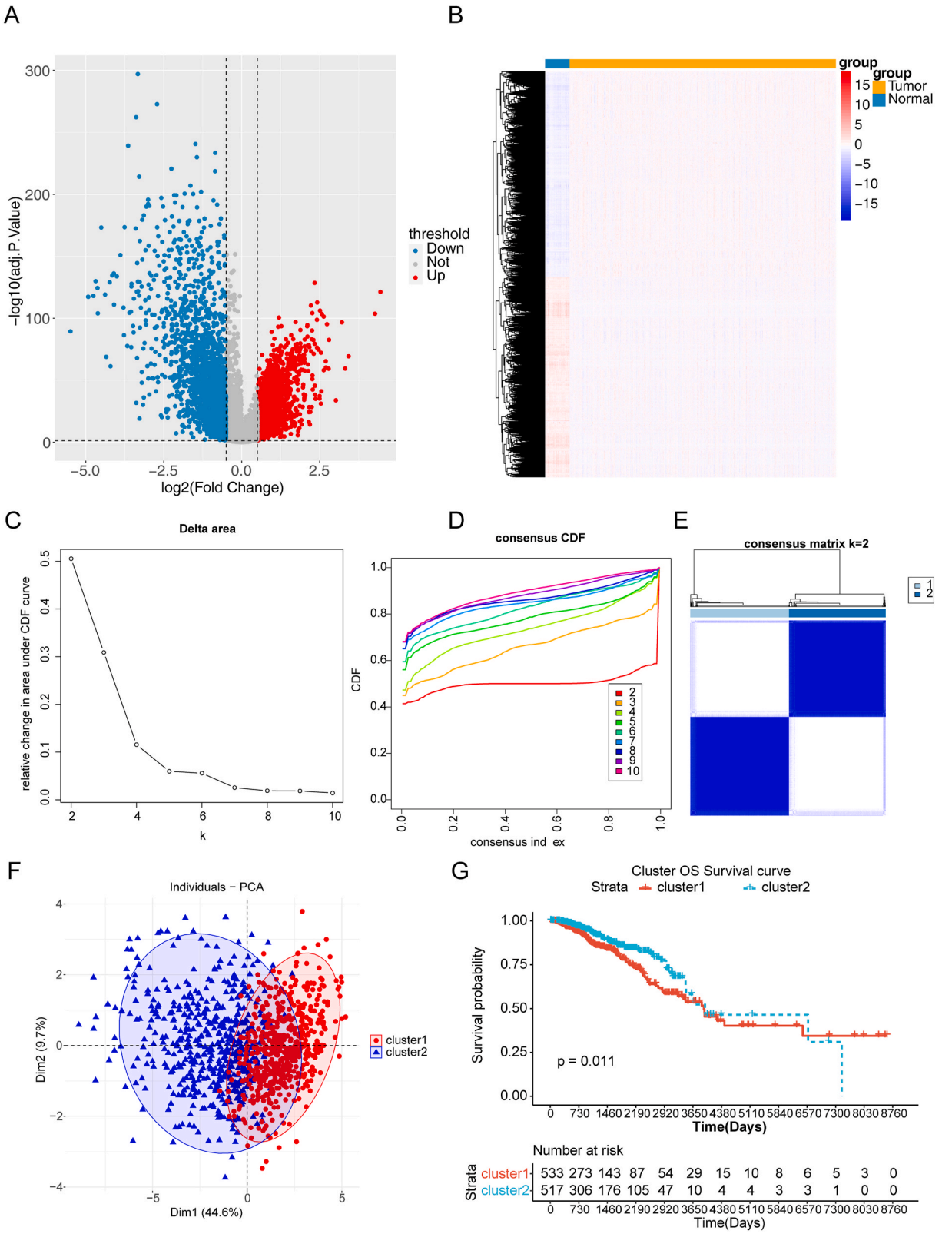

(caption on next page)

Fig. 1. Identification of two subgroups based on the immunogenic cell death-related genes (ICD-RGs) in TCGA-BRCA dataset. **(A)** Volcano map and **(B)** Heatmap of 4876 differentially expressed genes (DEGs) between the BRCA and normal groups. **(C)** Delta area plot exhibited the relative change in area under the cumulative distribution function (CDF) curve comparing K and K-1 (K ranges from two to ten), and the relative increases in consensus are used to determine K at which there is an appreciable increase. **(D)** The CDF of the consensus matrix for each K (indicated by colors). **(E)** Clustering matrix in TCGA-BRCA dataset when k = 2. **(F)** Principal Component Analysis (PCA) diagram for distribution of two clusters. **(G)** Kaplan-meier (K–M) survival analysis of two clusters in TCGA-BRCA dataset.

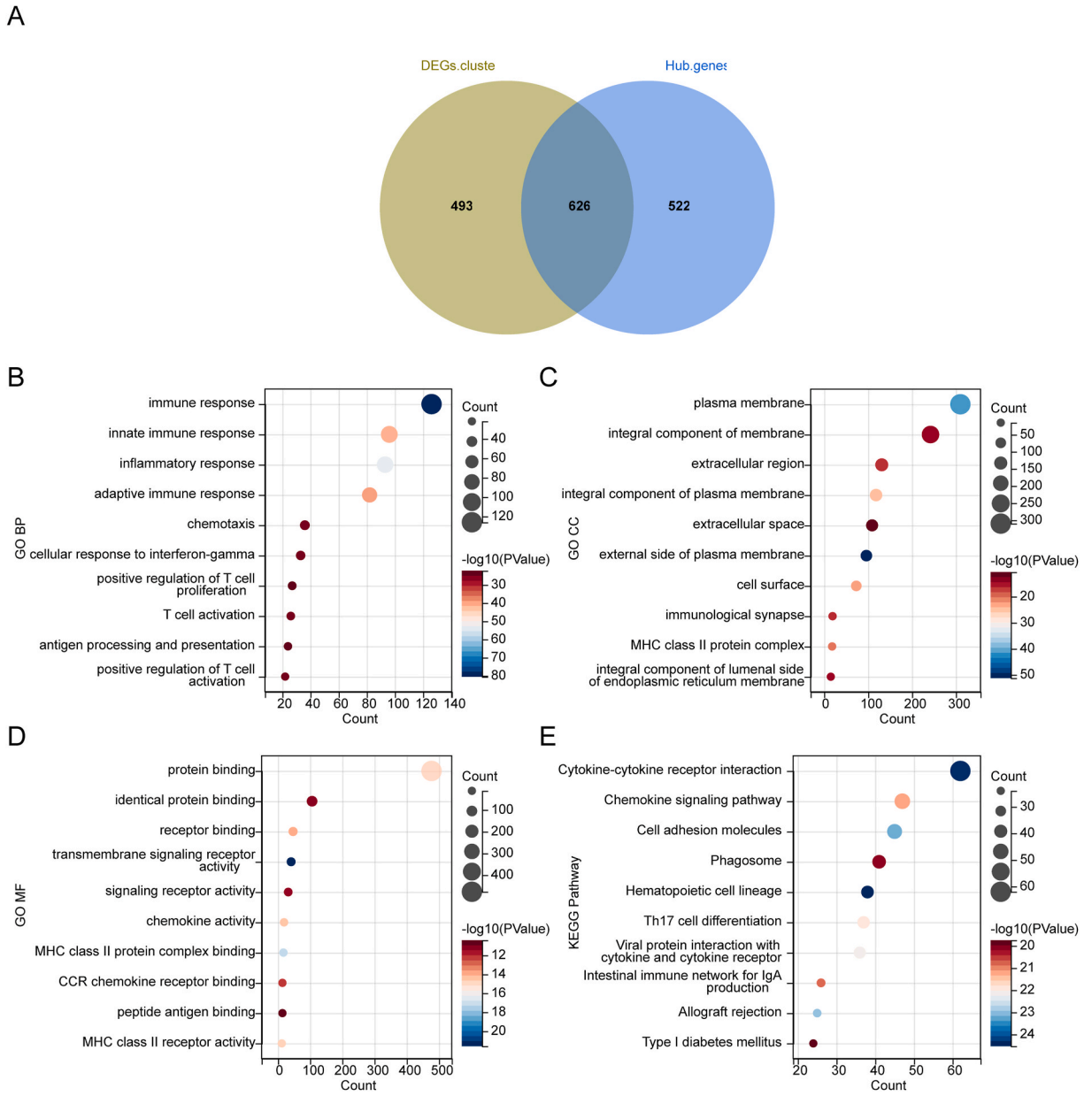

Fig. 2. Collection and functional enrichment analysis of the 626 intersecting genes. **(A)** Venn diagram for the intersecting genes common to DEGs between the Cluster1 and Cluster2 and key module genes. **(b–e)** Dot plot for the functions and pathways enriched by intersecting genes, including **(B)** gene ontology (GO)-biological process (BP), **(C)** cellular component (CC), **(D)** molecular function (MF) terms, and **(E)** Kyoto Encyclopedia of Genes and Genomes (KEGG) enrichment analyses.

was linked to functions like protein binding and chemokine activity (Fig. 2B–D). KEGG enrichment results included chemokine signaling pathway, etc. (Fig. 2E).

3.4. Biomarkers screening and risk model

A total of 989 target genes were identified through the Drugbank (n = 18), PubChem (n = 202), herb (n = 49), CTD (n = 1878), and batman (n = 70) databases (Table S1) after merging and de-duplication, and 33 candidate genes were obtained by overlapping intersecting genes, target genes, and DEGs between the BRCA and normal groups (Fig. 3A). Next, five ICD-PTX-related biomarkers (CHI3L1, IL18, PAPLN, SH2D2A, and UBE2L6) were acquired by univariate Cox analysis and LASSO (Fig. 3B–D).

Patients were divided into high-risk (n = 525) and low-risk groups (n = 525) based on the median value (−1.189112268) (Fig. 4A and B). Survival analysis demonstrated that the low-risk group in the training set exhibited a higher survival rate (P = 0.0014) (Fig. 4C). The ROC curve analysis displayed a good predictive performance of the model with AUC values exceeding 0.6 for 1-, 3-, and 5-year time points (Fig. 4D). Subsequently, an external validation cohort was used to assess the model's predictive capability. The result were consistent with the training set (P = 0.043) (Fig. 4E–G), and the AUC values for the validation cohort also exceeded 0.6 (Fig. 4H). Moreover, the cohorts with different clinical features (pathologic T, pathologic M, pathologic N, Age) were utilized for the K-M analysis as Table 2, and exhibited considerable difference in survival between two risk groups (Fig. S3).

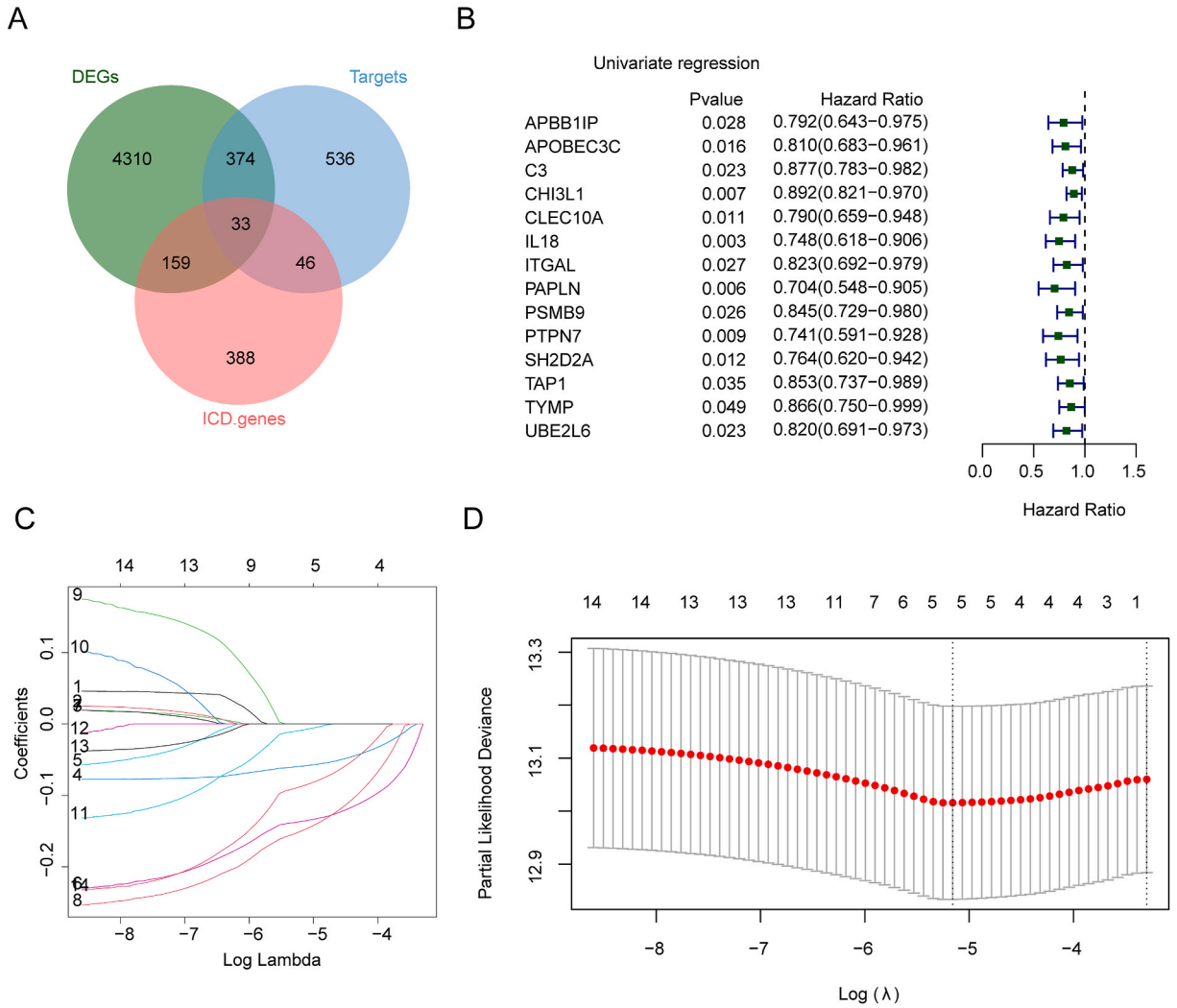

Fig. 3. Screening of five ICD-PTX-related biomarkers related to patient survival. **(A)** Venn diagram of 33 candidate genes. **(B)** Forest plot for the univariate Cox analysis to screen survival related candidate genes. **(C)** Least absolute shrinkage and selection operator (LASSO) coefficients profiles and **(D)** Cross-validation for tuning parameter selection.

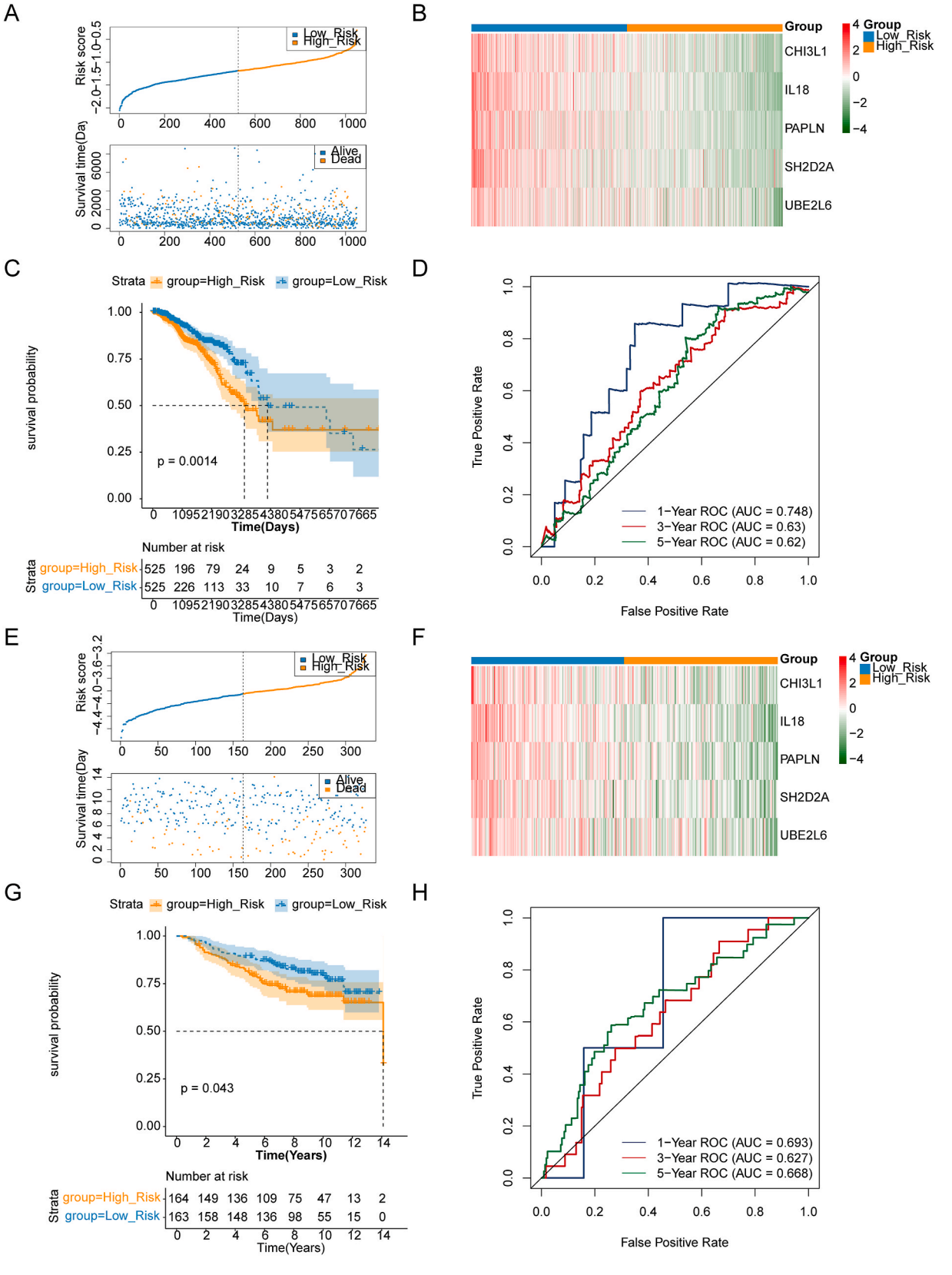

(caption on next page)

Fig. 4. Construction and validation of the risk model based on five ICD-PTX-related biomarkers. **(A)** Distribution of risk score, survival states and **(B)** gene expression of five biomarker genes in high risk group and low risk group from TCGA-BRCA dataset. **(C)** The K-M survival analysis of two risk groups in TCGA-BRCA dataset. (D) Receiver operating characteristic (ROC) curves of the risk model for survival prediction of TCGA-BRCA dataset at 1-, 3-, 5- years. **(E)** Distribution of risk score, survival states and **(F)** gene expression of five biomarker genes in two risk group from the external validation cohort (GSE20685 dataset). (**G**) The K-M survival analysis of two risk groups in GSE20685 dataset. (**H**) ROC curves of the risk model for survival prediction of patients in GSE20685 dataset at 1-, 3-, 5- years.

Table 2
The clinical information of TCGA cohorts in the high- and low-risk groups.

	Age		pathologic_T		pathologic_M		pathologic_N	
	>60	≤60	T1/T2	T3/T4	M0	M1	N0/N1	N2/N3
High risk	257	268	435	87	446	14	421	90
Low risk	205	320	446	76	433	8	421	101

3.5. Immune analysis between different risk groups

The bars displayed the distribution of 22 immune cell types (Fig. 5A). The box-plot displayed the presence of 16 differential types (memory B cells, Plasma cells, etc.) of immune infiltrating cells (Fig. 5B). In addition, the correlation analysis revealed that all the biomarkers except PAPLN were correlated with differential immune cells (adjusted $P < 0.05$ and $|r| > 0.3$) (Fig. 5C). SH2D2A exhibited the highest positive correlation with activated CD4 memory T cells and the strongest negative association with M2 Macrophages (Fig. 5D and E).

3.6. Single-gene GSEA analysis of biomarkers

The result of Single-gene GSEA showed that CHI3L1, IL18, SH2D2A, and UBE2L6 were mainly enriched in adaptive immune response, etc. GO-BP terms (Fig. S4A-B, Fig. S4D-E); PAPLN was mainly enriched in ATP synthesis coupled electron transport, DNA replication initiation and so on GO terms (Fig. S4C).

CHI3L1 and IL18 were found to enrich KEGG pathways such as hematopoietic cell lineage (Figs. S5A–B). PAPLN was mainly enriched to KEGG pathways such as DNA replication, hematopoietic cell lineage, etc. (Fig. S5C). SH2D2A and UBE2L6 were mainly enriched in autoimmune thyroid disease etc. KEGG pathway (Figs. S5D–E).

3.7. The ceRNA regulatory network of biomarkers

The 55 miRNAs targeting biomarkers were obtained through miRWalk3.0 and miRDB databases. Then, 13 targeting lncRNAs were predicted based on the above miRNAs. The network contained 5 biomarkers, 26 miRNAs and 13 lncRNAs (Fig. 6) were generated, including the interaction pairs of chr22-38_28785274-29006793.1-hsa-miR-765-SH2D2A, chr22-38_28785274-29006793.1-miR-197-IL-18, etc.

3.8. Expression analysis of biomarkers

The results of the expression of UBE2L6, IL18, and SH2D2A was higher in the BRCA group, while the opposite trend was observed for PAPLN and CHI3L1 (Fig. 7A). The qRT-PCR analysis was conducted to investigate the expression changes of biomarkers in both groups. The expression levels of IL8 and SH2D2A were notably lower in control samples compared to PTX-treated tissues, while CHI3L1 exhibited the opposite trend (Fig. 7B–D). There were no obvious differences in the expression levels of Papln and UBE2L6 between the two groups (Fig. 7E and F).

4. Discussion

BRCA is an immune heterogeneous disease that show great differences in different subtypes and individuals [4,7]. Anti-tumor immunity, which can effectively activate the immune system, is also one of the important factors in the selection of drugs for BRCA treatment [4]. ICD is a cell death process characterized by alterations in cell surface proteins and the release of soluble mediators. These changes stimulate phagocytes to present tumor antigens to immune cells like dendritic cells (DCs), macrophages, natural killer (NK) cells, and T cells [12,38,39]. By rendering tumor cells "visible" to the immune system, ICD triggers a robust anti-tumor response, especially through phagocytosis by DCs [12,38]. During ICD, tumor cells enhance the expression of calreticulin (CRT) on their surface, facilitating phagocytosis by DCs [12,40]. Additionally, the release of high-mobility-group box 1 (HMGB1) and ATP plays a crucial role in promoting DC chemotaxis, antigen presentation, and T cell activation [41–43]. Certain chemotherapy drugs, such as oxaliplatin (OXP), anthracyclines, and PTX, induce ICD, while others like cisplatin (CDDP) do not have this effect [12,17,21].

Targeting bioinformatics analysis to screen key differentially expressed genes and then conducting a series of functional analysis and prognosis studies has been used as a mature cancer analysis method, such as the utilize of multi-omics and single-cell data [44,45],

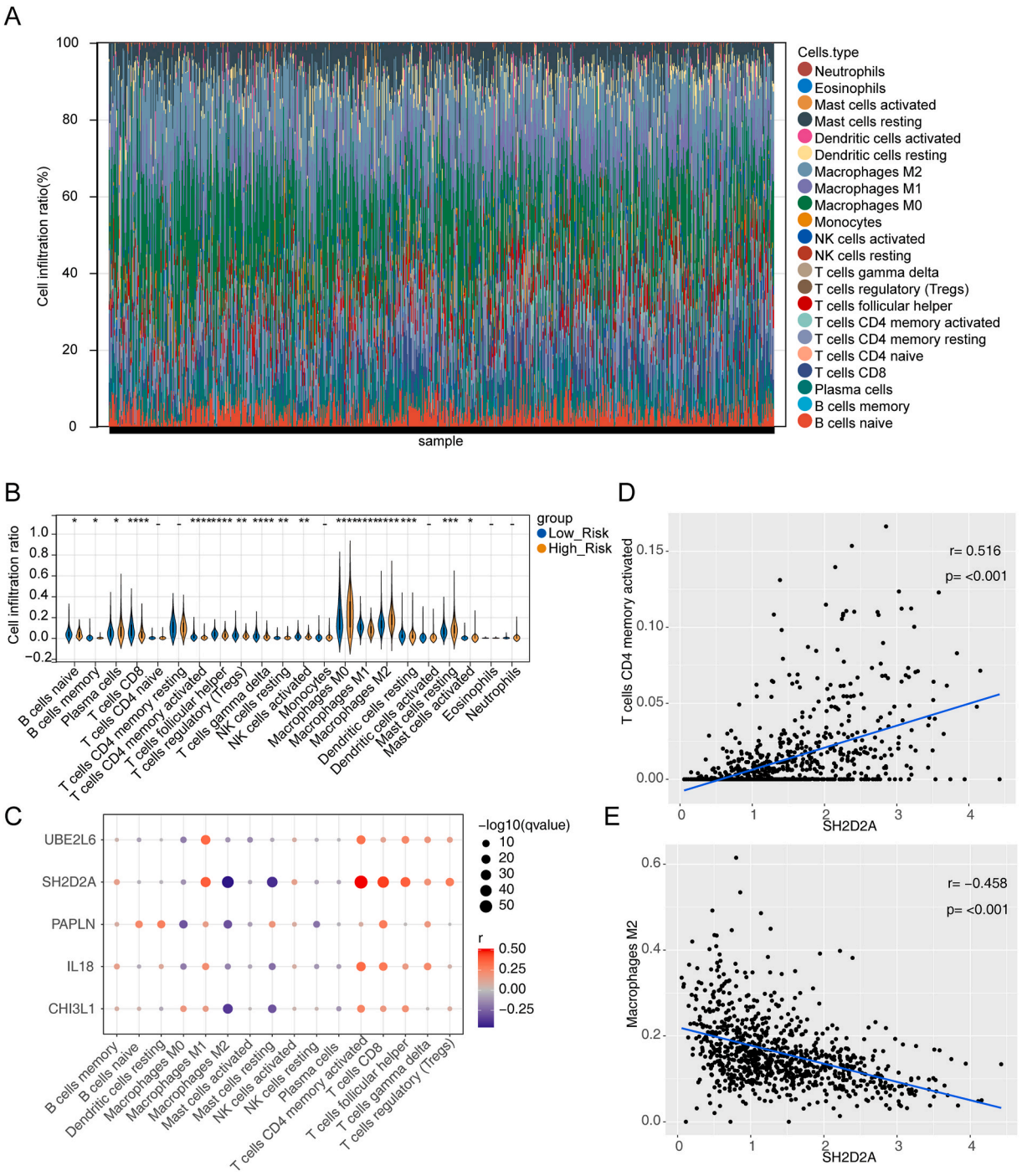

Fig. 5. Relationship of immune infiltration and risk model as well as biomarkers. **(A)** Histogram of 22 immune infiltration cells abundance in 1050 BRCA samples from the TCGA-BRCA dataset. **(B)** Violin plot for differences of the immune cell infiltration between two differential risk subgroups. $^{*}P < 0.05$, $^{**}P < 0.01$, $^{***}P < 0.001$, $^{****}P < 0.0001$, ns not significance. **(C)** Heatmap of the correlation between differential immune infiltration cells and five biomarkers. The bigger the circle, the stronger the correlation. Red indicates a positive correlation, while blue indicates a negative correlation. Scatter graph for the correlation of SH2D2A and **(D)** activated CD4 memory T cells and **(E)** M2 Macrophage.

likewise, the comprehensive evaluation of cell death-related genes for BRCA diagnosis [46]. Taking into account the previous anti-cancer evidence for the PTX-induced ICD mechanism in tumor cells [21,47], while the underlying mechanism as well as the target genes has not been systematically analyzed. In the present study, following up the results of the previous studies, we performed bioinformatics analysis of transcriptome data for normal breast tissue and BRCA samples in the UCSC Xene database, meanwhile the

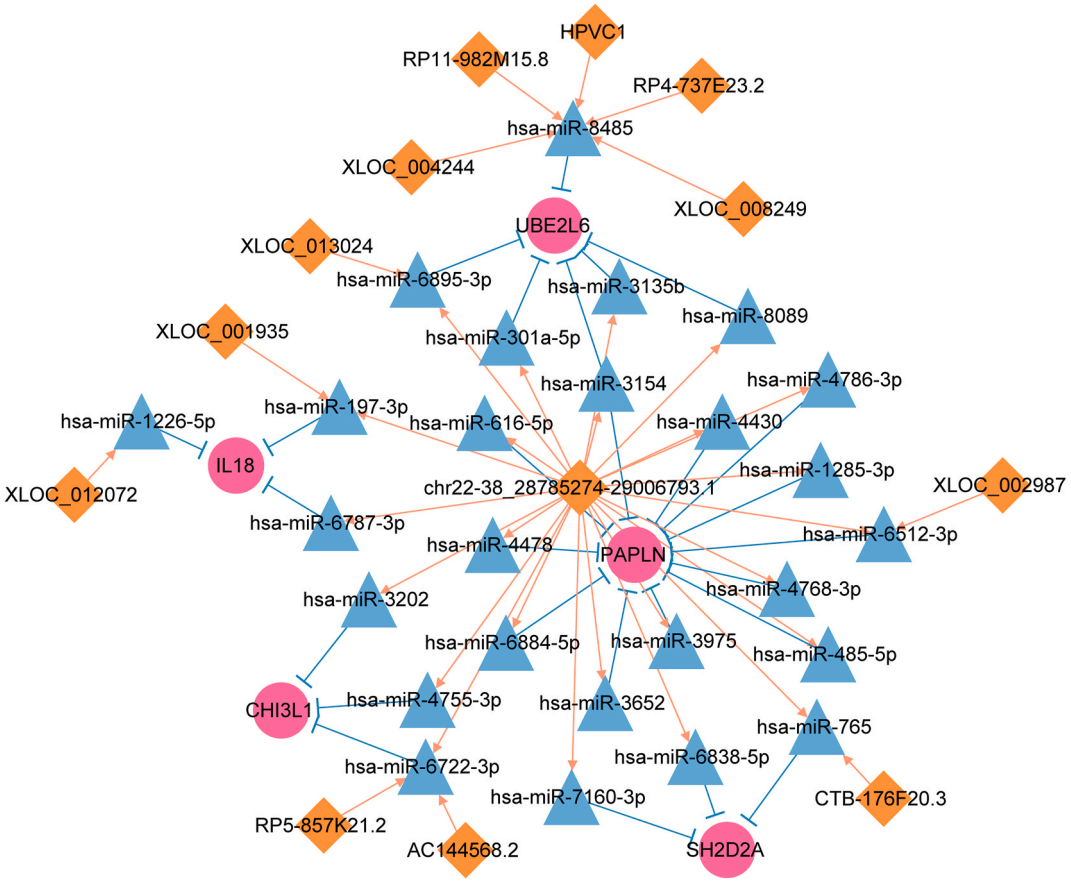

Fig. 6. The competing endogenous RNA (ceRNA) regulatory network of five biomarkers. The pink indicate mRNA, blue represent miRNA, and yellow symbolize lncRNA.

GSE20685 dataset was used as an external validation cohort. We screened the genes related to the anti-BRCA effect of PTX through ICD for the first time, and obtained 4 biomarkers (CHI3L1, PAPLN, SH2D2A, and UBE2L6) in the pathologies of BRCA as well as IL-18 to construct a risk model, where the prognostic value of IL-18 has been reported before [48].

Survival analysis and ROC analysis examined the moderate performance of the risk model for predicting prognosis of BRCA cohorts in the TCGA-BRCA and GSE20685 datasets. It is noteworthy that differences of sample size and follow-up time may affect the results of survival curve, where lost or invalid data are often excluded from K-M analysis, leading to potential selectivity bias. AUC results only reflect the prediction accuracy of the model when predicting whether an event occurs or not, but cannot provide information about survival time or survival probability. Considering the significant statistical significance of the model to a certain extent, more clinical samples need to be collected to further test the prognostic value of the model.

Next, the immune microenvironment analysis were carried out, and the results exhibited in the ceRNA regulatory network and functional enrichment results provide a new potential molecular mechanism for elucidating the ICD effect induced by PTX.

The SH2D2A gene encodes the T-cell-specific adapter protein (TSAd), which plays a role in regulating T-cell activation [49–51]. In BRCA1/2-negative high-risk families, the variation of signaling protein TSAd was positively correlated with the susceptibility to ovarian cancer [52]. Research in both mice and humans has suggested that the expression of TSAd in T cells is linked with the synthesis of IL-2 [53], which mainly stimulates the proliferation of T cells, cytotoxic T cells (CTLs) and NK cells, as well as enhances their killing activity and promotes lymphocytes secretion of antibodies and interferon. And meanwhile, TSAd also enhances synapse formation between $CD4^+$ T cells and APCs, influencing the differentiation of activated T cells by guiding the polarization of $CD4^+$ T cells towards the APC [54], and it enhances CD28-dependent costimulation [55]. The impact of SH2D2A in BCRA was firstly reported in this study. In our research, there is a strong correlation between SH2D2A expression and NK cells (negative) as well as activated $CD4^+$ memory T cells (positive), while the level of NK cells and activated $CD4^+$ memory T cells in the high-risk group is lower, indicating a negative correlation with the risk score. Our results show that SH2D2A expression was increased in BCRA samples, whereas the expression may be slightly lower with the increase of risk score, and meanwhile the expression level of SH2D2A is significantly up-regulated after PTX treatment, which is highly likely one of the intrinsic molecular mechanisms by which PTX induces ICD effect and promotes T cell activation.

Interleukin-18 (IL-18) is a potent stimulator of type-1 immune responses in both innate and adaptive lymphocytes [56]. Dendritic

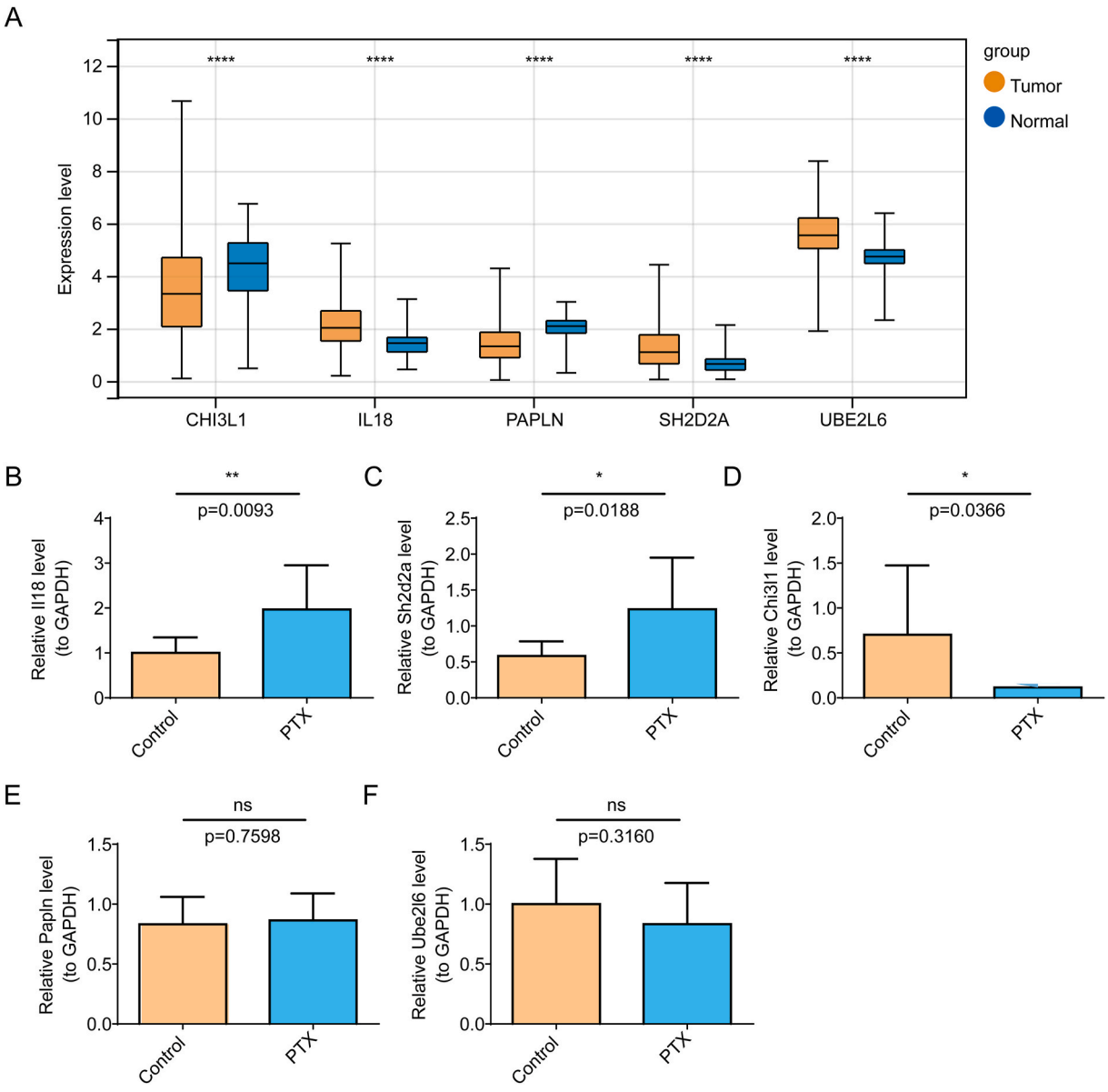

Fig. 7. Expression verification of five biomarkers. **(A)** Box plots for differences of the gene expression extracted from TCGA-BRCA dataset. **(B–F)** Results for mRNA level of five biomarkers using quantitative real-time polymerase chain reaction (qRT-PCR). $^{*}P < 0.05$, $^{**}P < 0.01$, ns not significance.

cells and macrophages are the main producers of active IL-18 [57], the significant alteration of these immune cell infiltration was observed in the tumor groups in this study. IL-18 receptor (IL-18R) is found on various cell types, including T cells, NK cells, peripheral B cells, macrophages, as well as non-immune cells like endothelial cells, epithelial cells, and fibroblasts [58]. IL-18 can enhance the lytic activity of NK cells [59], which not only promote the cytotoxicity of NK cells mediated by Fas-FasL ligand, but also promotes the traditional killing activity of perforin-mediated NK cells against target cells [59]. On the other hand, IL-18R serves as a new modulator of NK cell activity against tumors and viral infections by dampening the IL-18 pathway and facilitating IL-37-induced suppression of NK cells [60,61]. Our previous in vitro experiment results demonstrated that PTX-treated tumor cells conferred higher IL-18 secretion of BMDCs and were easier phagocytosed and presented by DCs and macrophages [21]. In addition, the IL-18 level of tumor tissue remarkable increased after PTX administration, echoing the high expression of IL-18 in patients with low risk group, which probably be an evidence for its activation of the immune system through the ICD effect. However, In cancer, inflammasomes and IL-18 can act as two-sided blades, as their activation may either fuel tumor growth and progression or conversely, bolster anti-tumor defense mechanisms and constrain tumor expansion [56,62–64]. High serum levels of IL-18 in some cancers and cancer-associated polymorphisms seem to escape from the immune system by suppressing CD70, while promoting metastasis by up-regulating of VEGF and CD44 [65].

Our bioinformatics analysis results showed that tumor tissue has a higher level of IL-18 mRNA than normal breast tissue, which also confirms the complexity and versatility of its regulation in the human immune system.

Non-enzymatic chitinase-3 like-protein-1 (CHI3L1) is a member of the glycoside hydrolase family 18, and is produced and released by various cell types such as macrophages, neutrophils, chondrocytes, fibroblast-like cells, endothelial cells, and cancer cells [66]. CHI3L1 appears to play a role in the proliferation, migration, and neoplastic advancement of colonic epithelial cells (CECs) in the presence of inflammatory conditions [67]. Macrophages and neutrophils present in the tumor microenvironment surrounding tumor cells have been observed to release CHI3L1 into the extracellular space. This protein can potentially boost tumor initiation, growth, angiogenesis, and metastasis [68]. Furthermore, studies have indicated that the upregulation of CHI3L1 signaling can alter the immunosuppressive environment by influencing the polarization of tumor-associated macrophages (TAMs). This alteration is controlled by a transcriptional program involving NF-κB/CEBPβ within the CHI3L1/Gal3-PI3K/AKT/mTOR axis or through a STAT6-dependent mechanism [69–71]. High levels of CHI3L1 expression have been linked to reduced survival rates in cancer patients. Specifically, in individuals with BRCA, increased CHI3L1 expression is associated with poorer survival outcomes, as demonstrated by analyses from KMplot and CGGA datasets [66]. Therefore, CHI3L1 may be one of the more promising prognostic markers for BRCA. After PTX treatment, the mRNA of CHI3L1 has been significantly degraded, which may indicate that its mechanism of ICD may be related to the above-mentioned pathway, and we will further explore it.

The enzyme UBE2L6, involved in protein ISGylation and ubiquitylation processes that control protein stability, has been identified as a novel inhibitor of autophagy. In esophageal cancer cells, UBE2L6 may impact chemosensitivity. Elevated UBE2L6 expression has been correlated with improved overall survival, possibly through enhancing apoptosis and suppressing autophagy. However, it is unclear whether this association with patient outcomes exists [72]. Furthermore, UBE2L6 is thought to play a significant role in tuberculosis by influencing apoptosis in macrophages infected with Mtb [73]. In human breast cells, UBE2L6 down-regulation was noted following the knockdown of BRCA2, a tumor suppressor protein with various functions. This down-regulation may be linked to the metabolism of ubiquitin cross-reacting protein (UCRP) [74]. For the first time, we found that UBE2L6 is up-regulated in BRCA tissues, and its detailed mechanism remains to be explored.

Proteoglycan-like sulfated glycoprotein (PAPLN), as known as papilin, is a component of the extracellular matrix [75]. In an integrative pan-cancer analysis, it was found that PAPLN was often linked to a positive prognosis, especially in terms of heightened sensitivity to certain drugs like erlotinib and osimertinib [76]. Simultaneously, PAPLN exhibited a positive correlation with immune checkpoint molecules such as Programmed Cell Death 1 Ligand 2 (PDCD1LG2) (PD-L2), Programmed Cell Death 1 (PDCD1) (PD-1), Cytotoxic T-Lymphocyte Associated Protein 4 (CTLA4), and Lymphocyte Activating 3 (LAG-3), suggesting its potential as targets and/or immune modulators for cancer therapy [76]. Experimental research on this gene is very limited, the detailed biological function of it in BRCA remains to be investigated.

The analysis of different immune cell types in different risk groups in our study has outstanding clinical implications. Comprehending the immune cell infiltration in tumor tissue is crucial for predicting disease progression and patient prognosis. By analyzing the correlation between key genes and immune cell infiltration, we can develop new therapeutic methods targeting key differential immune cells and even their additional related genes, or predict patients' response and sensitivity to specific therapies (such as immune checkpoint inhibitor therapy). In addition, different information of immune infiltration helps us to divide patients into subgroups with different immune characteristics for guiding individualized treatment strategies.

From the perspective of correlation of potential miRNAs related to the key genes predicted in this study, an in vitro experiment indicated that miR-765-3p may be located on the key regulatory axis of proteasome inhibitors in breast cancer cells, which affected the diversity of pathways [77]. And meanwhile, it can affect the functionality of various key signaling pathways, such as MAPK and NF-κB, and regulation the proliferation, tumor growth, metastasis and chemosensitivity of breast cancer cells. miR-765-3p was also predicted in our findings. MiR-197 is an anti-inflammatory agent, which can inhibit inflammation-related pathways, and one of its targets is IL-18, which has also been confirmed in many disease models [78]. Our analysis revealed that both has-miR-765 and has-miR-197-3p were linked to 5 biomarkers through lncRNA chr22-38_28785274–29006793, indicating its important regulatory roles in BRCA. In addition, the chr22-38_28785274-29006793.1–miR-34a/c-5p–capn 6 axis and chr22-38_28785 274-29006793.1–miR-494-3p–slc9a 7 axis might regulate cellular activities involved by $CD4^+$ and $CD8^+$ T cell infiltration in BRCA, respectively [79]. This again corresponds to our results of immune infiltration analysis. It is indicated that lncRNA chr22-38_28785274–29006793, probably play a central role in PTX-induced ICD effect, and it may be a potential target for diagnosis and treatment of BRCA, which needs further exploration.

The current study is subject to certain limitations. Despite our efforts to incorporate a wide range of datasets, only the UCSC Xene database and the GSE20685 dataset were utilized. This scope is insufficient to provide a comprehensive and robust profile for elucidating the mechanism of PTX-induced ICD effect, related genes, and associated signaling pathways. At the same time, compared with BRCA sample number (1072), the normal sample number (99) is lower. We use glmFit function to control the potential confounding effect more accurately and provide more accurate statistical inference, so as to obtain more reliable difference expression results. Although the sample size discrepancy will not affect the robustness of the results, it is still necessary to further expand the collection of clinical samples to verify the expression of key genes and related mechanisms, which can make up for the imbalance of samples in public data sets. In addition, we have verified by 4T1 subcutaneous model in mice, and the results obtained require further experiments and verification. Due to the lack of direct correlation between diseases and key genes, we may face challenges such as the lack of known pathophysiological mechanisms, the lack of sufficient clinical samples and the need to explore suitable animal models, which need to be further analyzed in combination with our predicted molecular mechanism-related clues.

5. Conclusion

In summary, this research offers a thorough bioinformatics analysis of pivotal genes and signaling pathways involved in PTX's anti-BRCA effect via ICD. This study obtained five biomarkers for it, constructed a prognostic related risk model and conducted immune microenvironment analysis and functional enrichment analysis for BRCA, represent a gap in the research so far. Our study, for the first time, identifies potential therapeutic targets of PTX's ICD effect through comprehensive bioinformatics analysis. It provides a new reference for the mechanism research, treatment and prognosis of the BRCA.

Funding statement

This work was supported by the grant from Yunnan Basic Research Program Youth Project (No. 202101AU070072), Open Fund Project of Yunnan Provincial Key Laboratory of Pharmacology for Natural Products (No. YKLPNP-G2410), and the program Innovative Research Team in Science and Technology in Kunming Medical University (No. CXTD202003).

Ethics approval

This study was conducted in strict accordance with the recommendations in the guide for the Care and Use of Laboratory Animals of Kunming Medical University, and the ethics approval number is KMMU2020236. All efforts were made to minimize the suffering of the mice.

Consent to participate

Informed consent was obtained from all subjects involved in the study. Written informed consent has been obtained from the patients to publish this paper.

Consent for publication

Not applicable.

Data availability statement

The datasets utilized and assessed in this study can be accessed from the UCSC Xene database (https://xenabrowser.net) and the GEO database (https://www.ncbi.nlm.nih.gov/gds) under the identifier [GSE20685].

CRediT authorship contribution statement

Qianmei Yang: Writing – review & editing, Writing – original draft, Validation, Supervision, Project administration, Methodology, Funding acquisition, Conceptualization. **Guimei Yang:** Writing – original draft, Project administration, Methodology, Conceptualization. **Yi Wu:** Writing – review & editing, Formal analysis, Data curation. **Lun Zhang:** Writing – review & editing, Methodology, Formal analysis, Data curation. **Zhuoyang Song:** Formal analysis, Data curation. **Dan Yang:** Writing – review & editing, Validation, Data curation.

Declaration of competing interest

The authors declare that they have no known competing financial interests or personal relationships that could have appeared to influence the work reported in this paper.

Appendix A. Supplementary data

Supplementary data to this article can be found online at https://doi.org/10.1016/j.heliyon.2024.e28409.

References

[1] A.N. Giaquinto, H. Sung, K.D. Miller, J.L. Kramer, L.A. Newman, A. Minihan, A. Jemal, R.L. Siegel, Breast cancer statistics, CA Cancer J Clin 72 (6) (2022) 524–541, https://doi.org/10.3322/caac.21754, 2022.
[2] R.L. Siegel, K.D. Miller, N.S. Wagle, A. Jemal, Cancer statistics, CA Cancer J Clin 73 (1) (2023) 17–48, https://doi.org/10.3322/caac.21763, 2023.
[3] U. Veronesi, P. Boyle, A. Goldhirsch, R. Orecchia, G. Viale, Breast cancer, Lancet 365 (9472) (2005) 1727–1741, https://doi.org/10.1016/s0140-6736(05)66546-4.
[4] K. Barzaman, J. Karami, Z. Zarei, A. Hosseinzadeh, M.H. Kazemi, S. Moradi-Kalbolandi, E. Safari, L. Farahmand, Breast cancer: biology, biomarkers, and treatments, Int. Immunopharm. 84 (2020) 106535, https://doi.org/10.1016/j.intimp.2020.106535.

[5] R.M. Pfeiffer, Y. Webb-Vargas, W. Wheeler, M.H. Gail, Proportion of U.S. Trends in breast cancer incidence Attributable to long-term changes in risk factor distributions, Cancer Epidemiol. Biomarkers Prev. 27 (10) (2018) 1214–1222, https://doi.org/10.1158/1055-9965.Epi-18-0098.
[6] C. Criscitiello, C. Corti, Breast cancer genetics: Diagnostics and treatment, Genes 13 (9) (2022), https://doi.org/10.3390/genes13091593.
[7] D. Nagarajan, S.E.B. McArdle, Immune landscape of breast cancers, Biomedicines 6 (1) (2018), https://doi.org/10.3390/biomedicines6010020.
[8] J. Ben-Dror, M. Shalamov, A. Sonnenblick, The history of early breast cancer treatment, Genes 13 (6) (2022), https://doi.org/10.3390/genes13060960.
[9] F.A. Fisusi, E.O. Akala, Drug combinations in breast cancer therapy, Pharm. Nanotechnol. 7 (1) (2019) 3–23, https://doi.org/10.2174/2211738507666190122111224.
[10] K.L. Maughan, M.A. Lutterbie, P.S. Ham, Treatment of breast cancer, Am. Fam. Physician 81 (11) (2010) 1339–1346.
[11] J. Zhang, L. Li, H. Shang, Z. Feng, T. Chao, A molecular classification system for estimating radiotherapy response and anticancer immunity for individual breast cancer patients, Front. Oncol. 13 (2023) 1288698, https://doi.org/10.3389/fonc.2023.1288698.
[12] G. Kroemer, L. Galluzzi, O. Kepp, L. Zitvogel, Immunogenic cell death in cancer therapy, Annu. Rev. Immunol. 31 (2013) 51–72, https://doi.org/10.1146/annurev-immunol-032712-100008.
[13] L. Galluzzi, J. Humeau, A. Buqué, L. Zitvogel, G. Kroemer, Immunostimulation with chemotherapy in the era of immune checkpoint inhibitors, Nat. Rev. Clin. Oncol. 17 (12) (2020) 725–741, https://doi.org/10.1038/s41571-020-0413-z.
[14] C.R. Gil Del Alcazar, M. Alečković, K. Polyak, Immune escape during breast tumor progression, Cancer Immunol. Res. 8 (4) (2020) 422–427, https://doi.org/10.1158/2326-6066.Cir-19-0786.
[15] E. Beyranvand Nejad, T.C. van der Sluis, S. van Duikeren, H. Yagita, G.M. Janssen, P.A. van Veelen, C.J. Melief, S.H. van der Burg, R. Arens, Tumor eradication by cisplatin is sustained by CD80/86-mediated costimulation of CD8+ T cells, Cancer Res. 76 (20) (2016) 6017–6029, https://doi.org/10.1158/0008-5472.Can-16-0881.
[16] T.C. van der Sluis, S. van Duikeren, S. Huppelschoten, E.S. Jordanova, E. Beyranvand Nejad, A. Sloots, L. Boon, V.T. Smit, M.J. Welters, F. Ossendorp, B. van de Water, R. Arens, S.H. van der Burg, C.J. Melief, Vaccine-induced tumor necrosis factor-producing T cells synergize with cisplatin to promote tumor cell death, Clin. Cancer Res. 21 (4) (2015) 781–794, https://doi.org/10.1158/1078-0432.Ccr-14-2142.
[17] A. Tesniere, F. Schlemmer, V. Boige, O. Kepp, I. Martins, F. Ghiringhelli, L. Aymeric, M. Michaud, L. Apetoh, L. Barault, J. Mendiboure, J.P. Pignon, V. Jooste, P. van Endert, M. Ducreux, L. Zitvogel, F. Piard, G. Kroemer, Immunogenic death of colon cancer cells treated with oxaliplatin, Oncogene 29 (4) (2010) 482–491, https://doi.org/10.1038/onc.2009.356.
[18] I. Martins, O. Kepp, F. Schlemmer, S. Adjemian, M. Tailler, S. Shen, M. Michaud, L. Menger, A. Gdoura, N. Tajeddine, A. Tesniere, L. Zitvogel, G. Kroemer, Restoration of the immunogenicity of cisplatin-induced cancer cell death by endoplasmic reticulum stress, Oncogene 30 (10) (2011) 1147–1158, https://doi.org/10.1038/onc.2010.500.
[19] E.B. Golden, D. Frances, I. Pellicciotta, S. Demaria, M. Helen Barcellos-Hoff, S.C. Formenti, Radiation fosters dose-dependent and chemotherapy-induced immunogenic cell death, OncoImmunology 3 (2014) e28518, https://doi.org/10.4161/onci.28518.
[20] C. Pozzi, A. Cuomo, I. Spadoni, E. Magni, A. Silvola, A. Conte, S. Sigismund, P.S. Ravenda, T. Bonaldi, M.G. Zampino, C. Cancelliere, P.P. Di Fiore, A. Bardelli, G. Penna, M. Rescigno, The EGFR-specific antibody cetuximab combined with chemotherapy triggers immunogenic cell death, Nat. Med. 22 (6) (2016) 624–631, https://doi.org/10.1038/nm.4078.
[21] Q. Yang, G. Shi, X. Chen, Y. Lin, L. Cheng, Q. Jiang, X. Yan, M. Jiang, Y. Li, H. Zhang, H. Wang, Y. Wang, Q. Wang, Y. Zhang, Y. Liu, X. Su, L. Dai, M. Tang, J. Li, L. Zhang, Z. Qian, D. Yu, H. Deng, Nanomicelle protects the immune activation effects of Paclitaxel and sensitizes tumors to anti-PD-1 Immunotherapy, Theranostics 10 (18) (2020) 8382–8399, https://doi.org/10.7150/thno.45391.
[22] A. Turpin, C. Neuzillet, E. Colle, N. Dusetti, R. Nicolle, J. Cros, L. de Mestier, J.B. Bachet, P. Hammel, Therapeutic advances in metastatic pancreatic cancer: a focus on targeted therapies, Ther Adv Med Oncol 14 (2022) 17588359221118019, https://doi.org/10.1177/17588359221118019.
[23] J. Cai, Y. Hu, Z. Ye, L. Ye, L. Gao, Y. Wang, Q. Sun, S. Tong, J. Yang, Q. Chen, Immunogenic cell death-related risk signature predicts prognosis and characterizes the tumour microenvironment in lower-grade glioma, Front. Immunol. 13 (2022) 1011757, https://doi.org/10.3389/fimmu.2022.1011757.
[24] M.D. Robinson, D.J. McCarthy, G.K. Smyth, edgeR: a Bioconductor package for differential expression analysis of digital gene expression data, Bioinformatics 26 (1) (2010) 139–140, https://doi.org/10.1093/bioinformatics/btp616.
[25] D.J. McCarthy, Y. Chen, G.K. Smyth, Differential expression analysis of multifactor RNA-Seq experiments with respect to biological variation, Nucleic Acids Res. 40 (10) (2012) 4288–4297, https://doi.org/10.1093/nar/gks042.
[26] M.D. Wilkerson, D.N. Hayes, ConsensusClusterPlus: a class discovery tool with confidence assessments and item tracking, Bioinformatics 26 (12) (2010) 1572–1573, https://doi.org/10.1093/bioinformatics/btq170.
[27] P. Langfelder, S. Horvath, WGCNA: an R package for weighted correlation network analysis, BMC Bioinf. 9 (2008) 559, https://doi.org/10.1186/1471-2105-9-559.
[28] G. Dennis Jr., B.T. Sherman, D.A. Hosack, J. Yang, W. Gao, H.C. Lane, R.A. Lempicki, DAVID: database for annotation, visualization, and integrated discovery, Genome Biol. 4 (5) (2003) P3.
[29] Y. Ye, Q. Dai, H. Qi, A novel defined pyroptosis-related gene signature for predicting the prognosis of ovarian cancer, Cell Death Dis. 7 (1) (2021) 71, https://doi.org/10.1038/s41420-021-00451-x.
[30] S. Qi, Y. Zhang, H. Gu, F. Zhu, M. Gao, H. Liang, Q. Zhang, Y. Gao, Machine learning and statistical models for analyzing multilevel patent data, Sci. Rep. 13 (1) (2023) 12783, https://doi.org/10.1038/s41598-023-37922-3.
[31] L. Feng, R. Hancock, C. Watson, R. Bogley, Z.A. Miller, M.L. Gorno-Tempini, M.J. Briggs-Gowan, F. Hoeft, Development of an abbreviated adult reading history Questionnaire (ARHQ-Brief) using a machine learning approach, J. Learn. Disabil. 55 (5) (2022) 427–442, https://doi.org/10.1177/00222194211047631.
[32] K. Ito, D. Murphy, Application of ggplot2 to Pharmacometric graphics, CPT Pharmacometrics Syst. Pharmacol. 2 (10) (2013) e79, https://doi.org/10.1038/psp.2013.56.
[33] J. In, D.K. Lee, Survival analysis: part II - applied clinical data analysis, Korean J Anesthesiol 72 (5) (2019) 441–457, https://doi.org/10.4097/kja.19183.
[34] A.M. Newman, C.L. Liu, M.R. Green, A.J. Gentles, W. Feng, Y. Xu, C.D. Hoang, M. Diehn, A.A. Alizadeh, Robust enumeration of cell subsets from tissue expression profiles, Nat. Methods 12 (5) (2015) 453–457, https://doi.org/10.1038/nmeth.3337.
[35] T. Wu, E. Hu, S. Xu, M. Chen, P. Guo, Z. Dai, T. Feng, L. Zhou, W. Tang, L. Zhan, X. Fu, S. Liu, X. Bo, G. Yu, clusterProfiler 4.0: a universal enrichment tool for interpreting omics data, Innovation 2 (3) (2021) 100141, https://doi.org/10.1016/j.xinn.2021.100141.
[36] G. Su, J.H. Morris, B. Demchak, G.D. Bader, Biological network exploration with Cytoscape 3, Curr Protoc Bioinformatics 47 (2014) 8.13.11–24, https://doi.org/10.1002/0471250953.bi0813s47.
[37] K.J. Livak, T.D. Schmittgen, Analysis of relative gene expression data using real-time quantitative PCR and the 2(-Delta Delta C(T)) Method, Methods 25 (4) (2001) 402–408, https://doi.org/10.1006/meth.2001.1262.
[38] A.D. Garg, L. Vandenberk, C. Koks, T. Verschuere, L. Boon, S.W. Van Gool, P. Agostinis, Dendritic cell vaccines based on immunogenic cell death elicit danger signals and T cell-driven rejection of high-grade glioma, Sci. Transl. Med. 8 (328) (2016) 328ra327, https://doi.org/10.1126/scitranslmed.aae0105.
[39] L. Galluzzi, A. Buque, O. Kepp, L. Zitvogel, G. Kroemer, Immunogenic cell death in cancer and infectious disease, Nat. Rev. Immunol. 17 (2) (2017) 97–111, https://doi.org/10.1038/nri.2016.107.
[40] D.V. Krysko, A.D. Garg, A. Kaczmarek, O. Krysko, P. Agostinis, P. Vandenabeele, Immunogenic cell death and DAMPs in cancer therapy, Nat. Rev. Cancer 12 (12) (2012) 860–875, https://doi.org/10.1038/nrc3380.
[41] G.P. Sims, D.C. Rowe, S.T. Rietdijk, R. Herbst, A.J. Coyle, HMGB1 and RAGE in inflammation and cancer, Annu. Rev. Immunol. 28 (2010) 367–388, https://doi.org/10.1146/annurev.immunol.021908.132603.
[42] L. Apetoh, F. Ghiringhelli, A. Tesniere, A. Criollo, C. Ortiz, R. Lidereau, C. Mariette, N. Chaput, J.P. Mira, S. Delaloge, F. Andre, T. Tursz, G. Kroemer, L. Zitvogel, The interaction between HMGB1 and TLR4 dictates the outcome of anticancer chemotherapy and radiotherapy, Immunol. Rev. 220 (2007) 47–59, https://doi.org/10.1111/j.1600-065X.2007.00573.x.

[43] M. Idzko, H. Hammad, M. van Nimwegen, M. Kool, M.A. Willart, F. Muskens, H.C. Hoogsteden, W. Luttmann, D. Ferrari, F. Di Virgilio, J.C. Virchow Jr., B. N. Lambrecht, Extracellular ATP triggers and maintains asthmatic airway inflammation by activating dendritic cells, Nat. Med. 13 (8) (2007) 913–919, https://doi.org/10.1038/nm1617.
[44] Z. Xing, D. Lin, Y. Hong, Z. Ma, H. Jiang, Y. Lu, J. Sun, J. Song, L. Xie, M. Yang, X. Xie, T. Wang, H. Zhou, X. Chen, X. Wang, J. Gao, Construction of a prognostic 6-gene signature for breast cancer based on multi-omics and single-cell data, Front. Oncol. 13 (2023) 1186858, https://doi.org/10.3389/fonc.2023.1186858.
[45] X. Tang, B. Ping, Y. Liu, Y. Zhou, Novel disulfidptosis-derived gene blueprint stratifying patients with breast cancer, Environ. Toxicol. (2023), https://doi.org/10.1002/tox.24043.
[46] X. Shi, H. Ding, J. Tao, Y. Zhu, X. Zhang, G. He, J. Yang, X. Wu, X. Liu, X. Yu, Comprehensive evaluation of cell death-related genes as novel diagnostic biomarkers for breast cancer, Heliyon 9 (11) (2023) e21341, https://doi.org/10.1016/j.heliyon.2023.e21341.
[47] J. Zhai, X. Gu, Y. Liu, Y. Hu, Y. Jiang, Z. Zhang, Chemotherapeutic and targeted drugs-induced immunogenic cell death in cancer models and antitumor therapy: an update review, Front. Pharmacol. 14 (2023) 1152934, https://doi.org/10.3389/fphar.2023.1152934.
[48] Y. Zhou, J. Zheng, M. Bai, Y. Gao, N. Lin, Effect of pyroptosis-related genes on the prognosis of breast cancer, Front. Oncol. 12 (2022) 948169, https://doi.org/10.3389/fonc.2022.948169.
[49] P. Borowicz, H. Chan, A. Hauge, A. Spurkland, Adaptor proteins: flexible and dynamic modulators of immune cell signalling, Scand. J. Immunol. 92 (5) (2020) e12951, https://doi.org/10.1111/sji.12951.
[50] S. Granum, V. Sundvold-Gjerstad, K.Z. Dai, K.M. Kolltveit, K. Hildebrand, H.S. Huitfeldt, T. Lea, A. Spurkland, Structure function analysis of SH2D2A isoforms expressed in T cells reveals a crucial role for the proline rich region encoded by SH2D2A exon 7, BMC Immunol. 7 (2006) 15, https://doi.org/10.1186/1471-2172-7-15.
[51] P.E. Lapinski, J.A. Oliver, J.N. Bodie, F. Marti, P.D. King, The T-cell-specific adapter protein family: TSAd, ALX, and SH2D4A/SH2D4B, Immunol. Rev. 232 (1) (2009) 240–254, https://doi.org/10.1111/j.1600-065X.2009.00829.x.
[52] L. Kaplun, A.L. Fridman, W. Chen, N.K. Levin, S. Ahsan, N. Petrucelli, J.L. Barrick, R. Gold, S. Land, M.S. Simon, R.T. Morris, A.R. Munkarah, M.A. Tainsky, Variants in the signaling protein TSAd are associated with susceptibility to ovarian cancer in BRCA1/2 negative high risk families, Biomark. Insights 7 (2012) 151–157, https://doi.org/10.4137/bmi.S10815.
[53] F. Marti, P.E. Lapinski, P.D. King, The emerging role of the T cell-specific adaptor (TSAd) protein as an autoimmune disease-regulator in mouse and man, Immunol. Lett. 97 (2) (2005) 165–170, https://doi.org/10.1016/j.imlet.2004.10.019.
[54] G. Abrahamsen, V. Sundvold-Gjerstad, M. Habtamu, B. Bogen, A. Spurkland, Polarity of CD4+ T cells towards the antigen presenting cell is regulated by the Lck adapter TSAd, Sci. Rep. 8 (1) (2018) 13319, https://doi.org/10.1038/s41598-018-31510-6.
[55] X. Tai, M. Cowan, L. Feigenbaum, A. Singer, CD28 costimulation of developing thymocytes induces Foxp3 expression and regulatory T cell differentiation independently of interleukin 2, Nat. Immunol. 6 (2) (2005) 152–162, https://doi.org/10.1038/ni1160.
[56] M. Esmailbeig, A. Ghaderi, Interleukin-18: a regulator of cancer and autoimmune diseases, Eur. Cytokine Netw. 28 (4) (2017) 127–140, https://doi.org/10.1684/ecn.2018.0401.
[57] C.A. Dinarello, Interleukin 1 and interleukin 18 as mediators of inflammation and the aging process, Am. J. Clin. Nutr. 83 (2) (2006) 447s–455s, https://doi.org/10.1093/ajcn/83.2.447S.
[58] C.A. Dinarello, D. Novick, S. Kim, G. Kaplanski, Interleukin-18 and IL-18 binding protein, Front. Immunol. 4 (2013) 289, https://doi.org/10.3389/fimmu.2013.00289.
[59] A.M. Abel, C. Yang, M.S. Thakar, S. Malarkannan, Natural killer cells: development, maturation, and clinical utilization, Front. Immunol. 9 (2018) 1869, https://doi.org/10.3389/fimmu.2018.01869.
[60] M. Molgora, E. Bonavita, A. Ponzetta, F. Riva, M. Barbagallo, S. Jaillon, B. Popović, G. Bernardini, E. Magrini, F. Gianni, S. Zelenay, S. Jonjić, A. Santoni, C. Garlanda, A. Mantovani, IL-1R8 is a checkpoint in NK cells regulating anti-tumour and anti-viral activity, Nature 551 (7678) (2017) 110–114, https://doi.org/10.1038/nature24293.
[61] D. Sarhan, K.L. Hippen, A. Lemire, S. Hying, X. Luo, T. Lenvik, J. Curtsinger, Z. Davis, B. Zhang, S. Cooley, F. Cichocki, B.R. Blazar, J.S. Miller, Adaptive NK cells resist regulatory T-cell suppression driven by IL37, Cancer Immunol. Res. 6 (7) (2018) 766–775, https://doi.org/10.1158/2326-6066.Cir-17-0498.
[62] M. Fabbi, G. Carbotti, S. Ferrini, Context-dependent role of IL-18 in cancer biology and counter-regulation by IL-18BP, J. Leukoc. Biol. 97 (4) (2015) 665–675, https://doi.org/10.1189/jlb.5RU0714-360RR.
[63] Y. Huang, W. Xu, R. Zhou, NLRP3 inflammasome activation and cell death, Cell. Mol. Immunol. 18 (9) (2021) 2114–2127, https://doi.org/10.1038/s41423-021-00740-6.
[64] Z. Li, X. Yu, J. Werner, A.V. Bazhin, J.G. D'Haese, The role of interleukin-18 in pancreatitis and pancreatic cancer, Cytokine Growth Factor Rev. 50 (2019) 1–12, https://doi.org/10.1016/j.cytogfr.2019.11.001.
[65] G. Palma, A. Barbieri, S. Bimonte, M. Palla, S. Zappavigna, M. Caraglia, P.A. Ascierto, G. Ciliberto, C. Arra, Interleukin 18: friend or foe in cancer, Biochim. Biophys. Acta 1836 (2) (2013) 296–303, https://doi.org/10.1016/j.bbcan.2013.09.001.
[66] T. Zhao, Z. Su, Y. Li, X. Zhang, Q. You, Chitinase-3 like-protein-1 function and its role in diseases, Signal Transduct. Targeted Ther. 5 (1) (2020) 201, https://doi.org/10.1038/s41392-020-00303-7.
[67] A. Kamba, I.A. Lee, E. Mizoguchi, Potential association between TLR4 and chitinase 3-like 1 (CHI3L1/YKL-40) signaling on colonic epithelial cells in inflammatory bowel disease and colitis-associated cancer, Curr. Mol. Med. 13 (7) (2013) 1110–1121, https://doi.org/10.2174/1566524011313070006.
[68] A.A. Abd El-Fattah, N.A.H. Sadik, O.G. Shaker, A. Mohamed Kamal, Single Nucleotide polymorphism in SMAD7 and CHI3L1 and Colorectal cancer risk, Mediat. Inflamm. 2018 (2018) 9853192, https://doi.org/10.1155/2018/9853192.
[69] Y. Chen, S. Zhang, Q. Wang, X. Zhang, Tumor-recruited M2 macrophages promote gastric and breast cancer metastasis via M2 macrophage-secreted CHI3L1 protein, J. Hematol. Oncol. 10 (1) (2017) 36, https://doi.org/10.1186/s13045-017-0408-0.
[70] A. Chen, Y. Jiang, Z. Li, L. Wu, U. Santiago, H. Zou, C. Cai, V. Sharma, Y. Guan, L.H. McCarl, J. Ma, Y.L. Wu, J. Michel, Y. Shi, L. Konnikova, N.M. Amankulor, P. O. Zinn, G. Kohanbash, S. Agnihotri, S. Lu, X. Lu, D. Sun, G.K. Gittes, Q. Wang, X. Xiao, D. Yimlamai, I.F. Pollack, C.J. Camacho, B. Hu, Chitinase-3-like 1 protein complexes modulate macrophage-mediated immune suppression in glioblastoma, J. Clin. Invest. 131 (16) (2021), https://doi.org/10.1172/jci147552.
[71] J. Huang, Z. Gu, Y. Xu, L. Jiang, W. Zhu, W. Wang, CHI3L1 (Chitinase 3 like 1) upregulation is associated with macrophage signatures in esophageal cancer, Bioengineered 12 (1) (2021) 7882–7892, https://doi.org/10.1080/21655979.2021.1974654.
[72] C.M. Falvey, T.R. O'Donovan, S. El-Mashed, M.J. Nyhan, S. O'Reilly, S.L. McKenna, UBE2L6/UBCH8 and ISG15 attenuate autophagy in esophageal cancer cells, Oncotarget 8 (14) (2017) 23479–23491, https://doi.org/10.18632/oncotarget.15182.
[73] J. Gao, C. Li, W. Li, H. Chen, Y. Fu, Z. Yi, Increased UBE2L6 regulated by type 1 interferon as potential marker in TB, J. Cell Mol. Med. 25 (24) (2021) 11232–11243, https://doi.org/10.1111/jcmm.17046.
[74] M.K. Tripathi, G. Chaudhuri, Down-regulation of UCRP and UBE2L6 in BRCA2 knocked-down human breast cells, Biochem. Biophys. Res. Commun. 328 (1) (2005) 43–48, https://doi.org/10.1016/j.bbrc.2004.12.142.
[75] K. Hotta, M. Kikuchi, T. Kitamoto, A. Kitamoto, Y. Ogawa, Y. Honda, T. Kessoku, K. Kobayashi, M. Yoneda, K. Imajo, W. Tomeno, A. Nakaya, Y. Suzuki, S. Saito, A. Nakajima, Identification of core gene networks and hub genes associated with progression of non-alcoholic fatty liver disease by RNA sequencing, Hepatol. Res. 47 (13) (2017) 1445–1458, https://doi.org/10.1111/hepr.12877.
[76] X. Zhang, W. Yang, K. Chen, T. Zheng, Z. Guo, Y. Peng, Z. Yang, The potential prognostic values of the ADAMTS-like protein family: an integrative pan-cancer analysis, Ann. Transl. Med. 9 (20) (2021) 1562, https://doi.org/10.21037/atm-21-4946.

[77] K. Katsaraki, C.K. Kontos, G. Ardavanis-Loukeris, A.A. Tzovaras, D.C. Sideris, A. Scorilas, Exploring the time-dependent regulatory potential of microRNAs in breast cancer cells treated with proteasome inhibitors, Clin. Transl. Oncol. (2023), https://doi.org/10.1007/s12094-023-03349-5.

[78] N. Asri, S. Fallah, M. Rostami-Nejad, Z. Fallah, M. Khanlari-Kochaksaraei, S. Jafari-Marandi, F. Forouzesh, S. Shahrokh, S. Jahani-Sherafat, M.R. Zali, The role of mir-197-3p in regulating the tight junction permeability of celiac disease patients under gluten free diet, Mol. Biol. Rep. 50 (3) (2023) 2007–2014, https://doi.org/10.1007/s11033-022-08147-w.

[79] Z. Wang, X. Yang, J. Shen, J. Xu, M. Pan, J. Liu, S. Han, Gene expression patterns associated with tumor-infiltrating CD4+ and CD8+ T cells in invasive breast carcinomas, Hum. Immunol. 82 (4) (2021) 279–287, https://doi.org/10.1016/j.humimm.2021.02.001.